REPORT

GNB5 Mutations Cause an Autosomal-Recessive Multisystem Syndrome with Sinus Bradycardia and Cognitive Disability

Elisabeth M. Lodder,[1,22] Pasquelena De Nittis,[2,3,22] Charlotte D. Koopman,[4,5,22] Wojciech Wiszniewski,[6] Carolina Fischinger Moura de Souza,[7] Najim Lahrouchi,[1] Nicolas Guex,[2,8] Valerio Napolioni,[9] Federico Tessadori,[5] Leander Beekman,[1] Eline A. Nannenberg,[10] Lamiae Boualla,[11] Nico A. Blom,[12] Wim de Graaff,[13] Maarten Kamermans,[13,14] Dario Cocciadiferro,[3,15] Natascia Malerba,[3,15] Barbara Mandriani,[3,16] Zeynep Hande Coban Akdemir,[6] Richard J. Fish,[17] Mohammad K. Eldomery,[6] Ilham Ratbi,[11] Arthur A.M. Wilde,[1] Teun de Boer,[4] William F. Simonds,[18] Marguerite Neerman-Arbez,[17] V. Reid Sutton,[6,19] Fernando Kok,[20] James R. Lupski,[6,19,21] Alexandre Reymond,[2,23] Connie R. Bezzina,[1,23] Jeroen Bakkers,[4,5,23,*] and Giuseppe Merla[3,23,*]

GNB5 encodes the G protein β subunit 5 and is involved in inhibitory G protein signaling. Here, we report mutations in *GNB5* that are associated with heart-rate disturbance, eye disease, intellectual disability, gastric problems, hypotonia, and seizures in nine individuals from six families. We observed an association between the nature of the variants and clinical severity; individuals with loss-of-function alleles had more severe symptoms, including substantial developmental delay, speech defects, severe hypotonia, pathological gastro-esophageal reflux, retinal disease, and sinus-node dysfunction, whereas related heterozygotes harboring missense variants presented with a clinically milder phenotype. Zebrafish *gnb5* knockouts recapitulated the phenotypic spectrum of affected individuals, including cardiac, neurological, and ophthalmological abnormalities, supporting a direct role of GNB5 in the control of heart rate, hypotonia, and vision.

Heterotrimeric G proteins trigger a signal transduction cascade composed of α, β, and γ subunits. They are associated with G protein-coupled receptors (GPCRs) in modulating an array of cellular functions, including release of a multitude of hormones and growth factors, regulation of cell contraction and migration, and cell growth and differentiation during development.[1–4] G protein-coupled signaling plays a crucial role in neuronal communication, including regulation of the antagonistic effects of the parasympathetic and sympathetic branches of the autonomic nervous system throughout the body. We report a genetic disorder caused by mutations affecting *GNB5* (MIM: 604447), encoding guanine nucleotide-binding protein subunit beta-5, and with disease manifestation in multiple systems.

We identified nine affected individuals (six females and three males) from six unrelated families presenting with a clinical overlap of neurological and cardiac conduction defects; all subjects were found to have variation in the same gene, *GNB5*, and share a similar rare phenotype. This work results from exome and phenotype data aggregation among independent groups engaged in studying the molecular basis of yet unsolved human genetic rare disease traits. Shared phenotypic features representing the cardinal characteristics of the syndrome include global developmental delay, seizures, generalized hypotonia, retinal disease, and the uncommon feature of early-onset sinus-node dysfunction (Table 1). Additional clinical investigations and diagnostic studies did not show any evidence of structural CNS, ocular, or cardiac anomalies. Affected individuals from four of the six families (families A–D) demonstrated the severe end of the disease spectrum, including substantial cognitive deficits, delayed motor development, severe

[1]Department of Clinical and Experimental Cardiology, Heart Center, Academic Medical Center, University of Amsterdam, 1105 AZ Amsterdam, the Netherlands; [2]Center for Integrative Genomics, University of Lausanne, 1015 Lausanne, Switzerland; [3]Medical Genetics Unit, IRCCS Casa Sollievo della Sofferenza, viale Cappuccini, 71013 San Giovanni Rotondo, Foggia, Italy; [4]Department of Medical Physiology, Division of Heart and Lungs, University Medical Center Utrecht, 3584 CT Utrecht, the Netherlands; [5]Hubrecht Institute– Royal Netherlands Academy of Arts and Sciences (KNAW), University Medical Centre Utrecht, 3584 CT Utrecht, the Netherlands; [6]Department of Molecular and Human Genetics, Baylor College of Medicine, Houston, TX 77030, USA; [7]Medical Genetics Service, Hospital de Clinicas de Porto Alegre, 2350 Porto Alegre, Brazil; [8]Swiss Institute of Bioinformatics, 1015 Lausanne, Switzerland; [9]Department of Neurology and Neurological Sciences, Stanford University School of Medicine, Palo Alto, CA 94304, USA; [10]Department of Clinical Genetics, Academic Medical Center, University of Amsterdam, 1105 AZ Amsterdam, the Netherlands; [11]Centre de Génomique Humaine, Faculté de Médecine et Pharmacie, Mohammed V University of Rabat, 8007, Rabat, Morocco; [12]Department of Pediatric Cardiology, Emma Children's Hospital, Academic Medical Centre, 1105 AZ Amsterdam, the Netherlands; [13]Retinal Signal Processing Lab, Netherlands Institute for Neuroscience, 1105 BA Amsterdam, the Netherlands; [14]Department of Genome Analysis, Academic Medical Center, University of Amsterdam, 1105 AZ Amsterdam, the Netherlands; [15]PhD Program in Experimental and Regenerative Medicine, Faculty of Medicine, University of Foggia, 71121 Foggia, Italy; [16]PhD Program in Molecular Genetics Applied to Medical Sciences, Department of Molecular and Translational Medicine, University of Brescia, 25121 Brescia, Italy; [17]Department of Genetic Medicine and Development, University Medical Centre (CMU), 1211 Geneva, Switzerland; [18]Metabolic Diseases Branch, National Institute of Diabetes and Digestive and Kidney Diseases, NIH, Bethesda, MD 20892-2560, USA; [19]Texas Children's Hospital, Houston, TX 77030, USA; [20]Child Neurology Division, Department of Neurology, School of Medicine, University of Sao Paulo, 01246903 Sao Paulo, Brazil; [21]Department of Pediatrics, Baylor College of Medicine, Houston, TX 77030, USA
[22]These authors contributed equally to this work
[23]These authors contributed equally to this work
*Correspondence: j.bakkers@hubrecht.eu (J.B.), g.merla@operapadrepio.it (G.M.)
http://dx.doi.org/10.1016/j.ajhg.2016.06.025.

Table 1. Overlapping Clinical Features of Individuals with *GNB5* Mutations

	Family A		Family B	Family C		Family D	Family E		Family F
	II.1	II.2	II.1	II.2	II.3	II.2	II.1	II.2	II.1
Gender, age (years)	F, 22	F, 20	F, 6	F, 11	M, 9	F, 12	F, 13	M, 8	M, 23
Birth weight	3,580 g (50^{th} percentile)	NA	2,980 g (15^{th} percentile)	2,751 g (15^{th} percentile)	NA	2,845 g (15^{th} percentile)	NA	NA	NA
Ethnicity	Italy	Italy	Jordan	Puerto Rico	Puerto Rico	India	Morocco	Morocco	Brazil
Consanguinity	–	–	+	+	+	–	–	–	+
Altered speech development	+	+	+	+	+	+	+	+	NA
Verbal understanding	NA	NA	nonverbal	unremarkable	unremarkable	NA	NA	NA	NA
Lexical production	NA	NA	nonverbal	delayed	delayed	nonverbal	delayed	delayed	NA
Intellectual disability	+	+	+	+	+	+	mild	mild	mild
Epilepsy	+	+	+	–	–	+	–	–	–
Sinus sick syndrome	+	+	+	+	+	increased PR interval (intermittent Weckenbach)	+	+	+
Minimum heart rate (bpm)	24	39	NA	paced	paced	NA	20	16	
Maximum heart rate (bpm)	163	192	NA	paced (27% heartbeats on Holter)	paced (20% heartbeats on Holter)	NA	176	180	NA
Chronotropic response	NA	NA	NA	+	+	NA	unremarkable	unremarkable	NA
Escape beats	+	+	NA	paced	paced	NA	+	+	NA
Pacemaker implantation	–	–	–	+	+	–	–	+	NA
Heart structural abnormalities	–	PFO	NA	–	–	–	–	–	NA
Hypotonia	+	+	+	+	+	+	–	impaired fine motor skills	–
Pathological gastric reflux	+	+	–	+	+	+	–	–	NA
Nystagmus	+	+	+	+	+	+	NA	–	NA
Plasma amino acids chromatography	938 μm/L (restored)	+ (restored)	unremarkable	unremarkable	unremarkable	unremarkable	444 μm/L	unremarkable	NA
Urine organic acids	unremarkable	unremarkable	increased excretion of 3-methyl-glutaconic acid	unremarkable	unremarkable	unremarkable	NA	NA	NA

Affected individual numbers refer to those in the pedigree in Figure 1. Complete pedigree charts, consanguinity status, variants, and related homozygous and/or compound heterozygous alleles are reported in Figure 1 and Table S1. Abbreviations are as follows: M, male; f, female; NA, not available; +, clinical trait present; –, clinical trait not present; PFO, patent foramen ovale; bpm, beats per minute.

hypotonia, retinal disease, pathological gastro-esophageal reflux, and sinus-node dysfunction. Affected individuals in families E and F presented with a milder phenotype, including mild intellectual impairment, language delay, and bradycardia (Figure 1, Table 1, Supplemental Note).

Given that no potentially pathogenic genomic structural abnormalities were identified by array comparative genomic hybridization and karyotyping of the affected subjects, we applied whole-exome sequencing to all the affected individuals and their healthy parents. Families were recruited in Italy (family A), Brazil (B and F), the United States (C and D), and the Netherlands (E). The institutional review boards of the IRCCS Casa Sollievo Della Sofferenza Hospital, the Hospital das Clínicas da Universidade de São Paulo, the

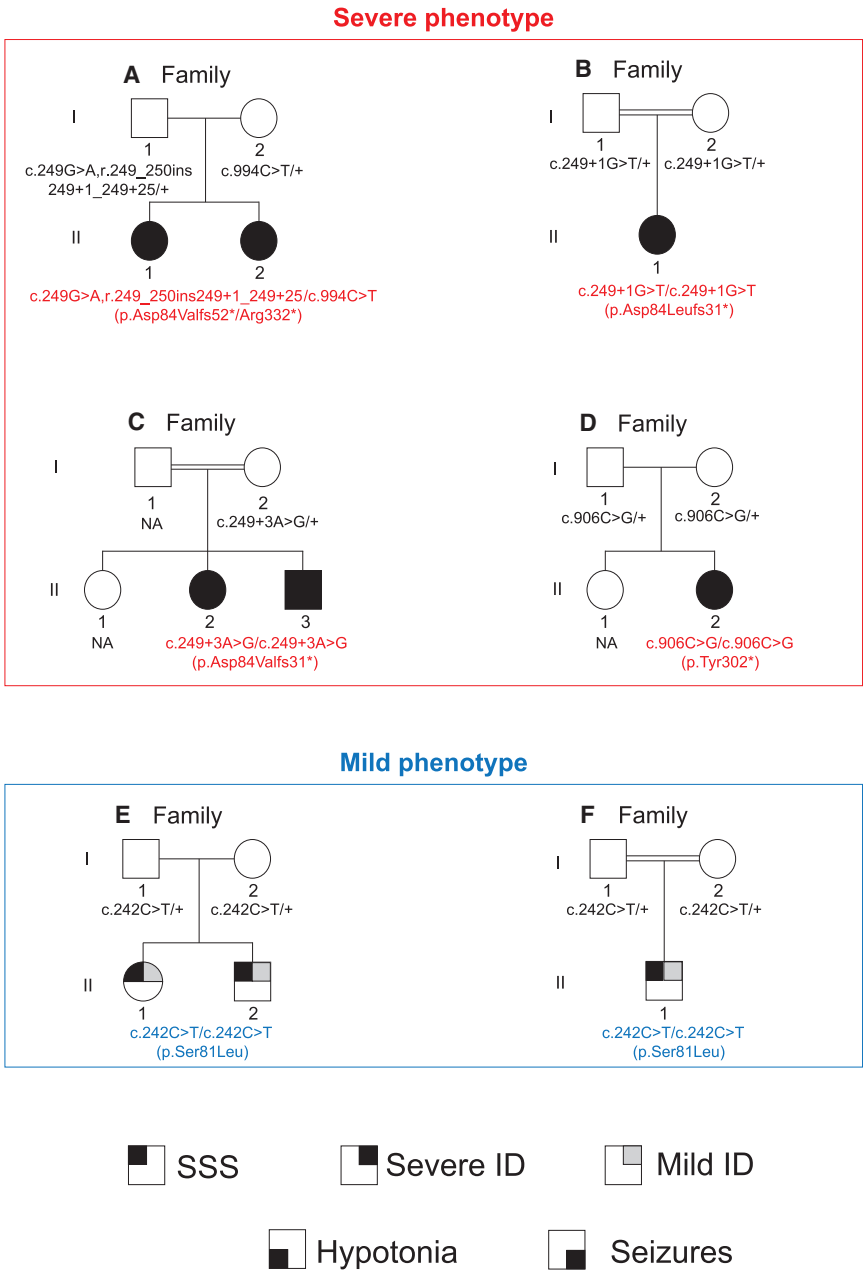

Figure 1. Pedigrees from the Six Families Investigated in this Study

Affected members of families A to D (upper red-lined panel) and E to F (lower blue-lined panel) show severe and mild manifestation of the core symptoms of the syndrome defined in this study. Filled symbols represent individuals with severe sinus sick syndrome (SSS; top left quarter), intellectual disability (ID; top right quarter), hypotonia (bottom left quarter), and seizures (bottom right quarter), whereas a light-gray top left quarter indicates the presence of mild ID. Genotypes are specified according to GenBank: NM_006578.3.

Baylor College of Medicine, the Amsterdam Academic Medical Center, and the University of Lausanne approved this study. Participants were enrolled after written informed consent was obtained from parents or legal guardians. The clinical evaluation included medical history interviews, a physical examination, and review of medical records. To uncover genetic variants associated with the complex phenotype shown by the nine affected subjects, we sequenced their exomes and those of their parents. DNA libraries were prepared from blood-derived genomic DNAs according to standard procedures. Exomes were captured and sequenced with different platforms to reach 50- to 120-fold coverage on average. Variants were called as previously described.[5–7] Variants were filtered on the basis of inheritance patterns, including autosomal recessive, X-linked, and de novo and/or autosomal dominant. Variants with MAF < 0.05% in control cohorts (dbSNP, the 1000 Genome Project, NHLBI GO Exome Sequencing Project, the Exome Aggregation Consortium database, and our in-house databases) and predicted to be deleterious by SIFT,[8] PolyPhen-2,[9] and/or UMD-Predictor[10] were prioritized.

Given a potential history of consanguinity reported in some families (families B, C, and F [Figure 1, Table 1]), we filtered variants by using Mendelian expectations for the assumption of a rare autosomal-recessive trait. We found *GNB5* to be compliant with Mendelian expectations and bearing bi-allelic putative deleterious variants in all affected individuals (Figure 1, Table S1). Sanger sequencing in each family confirmed the anticipated segregation of the *GNB5* variants. Strikingly, the variants found in the severely affected individuals (families A–D) were predicted to be loss-of-function (LoF) alleles, whereas the more mildly affected individuals from families E and F were homozygous for the same missense variant, c.242C>T (p.Ser81Leu [GenBank: NM_006578.3]) (Figures 1 and S1A). In families B, C, and D the affected individuals were homozygous for splice variants (c.249+1G>T [p.Asp84Leufs31*] and c.249G+3A>G [p.Asp84Valfs31*]) and a nonsense variant (c.906C>G [p.Tyr302*]), respectively (Figures 1 and S1A, Table S1). In family A, the affected siblings were compound heterozygous for a maternally inherited nonsense variant (c.994C>T [p.Arg332*]) and a paternally inherited splice-site change (c.249G>A [p.(=)]), which gives rise to an aberrantly spliced isoform containing an additional 25 nucleotides of the intervening intron 2 (Figure S2A). We experimentally show that the transcripts from both alleles are targeted by nonsense-mediated mRNA-decay (Figure S2B).

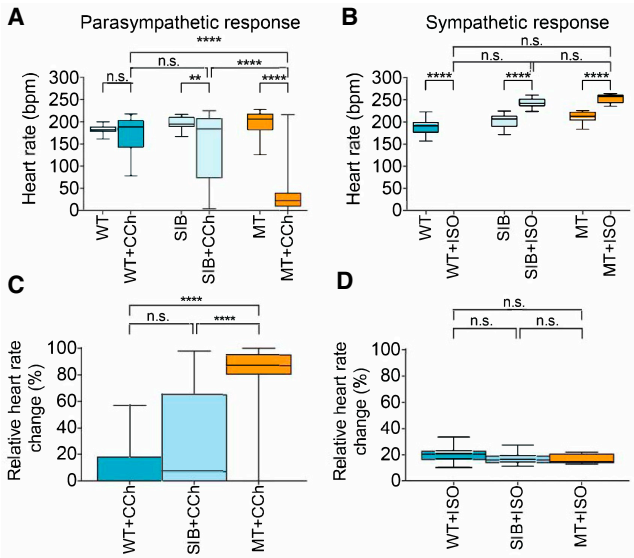

Figure 2. Cardiac Function in *gnb5* Mutant Zebrafish
(A–D) Box-whisker plots demonstrate the heart rate response and the relative heart rate change of 5 dpf wild-type (WT), sibling (SIB), and *gnb5* mutant (MT) larvae. Embryos at 5 dpf were embedded in 0.3% agarose prepared in E3 medium containing 16 mg/ml Tricaine. Basal heart rates were recorded first. Then, (A and C) 400 μM of the parasympathetic agonist carbachol (CCh; Sigma-Aldrich C4382) (WT n = 10, SIB n = 39, MT n = 14) or (B and D) 100 μM of the sympathetic agonist isoproterenol hydrochloride (ISO; Sigma-Aldrich 1351005) (WT n = 12, SIB n = 22, MT n = 9) was added and incubated for 30 min and heart rates were measured. Recordings were performed at 150 frames per second and were analyzed with ImageJ. The relative heart rate change is the percentage change between the basal heart rate measured and the heart rate after addition of CCh or ISO.
n denotes the number of fish used per dataset. Differences between two groups were analyzed via the Student's t test. Differences between more than two groups were analyzed via one-way ANOVA with Tukey's post-hoc test. Data are shown as mean ± SEM, and $p < 0.05$ was considered significant. *$p < 0.05$, **$p \leq 0.01$, ***$p \leq 0.001$, ****$p \leq 0.0001$. $p > 0.05$ was considered not significant (n.s.). bpm, beats per minute.

The five *GNB5* LoF variants identified in families A–D are either not present or present with MAF $\leq 8.25 \times 10^{-6}$ in ExAC (Exome Aggregation Consortium, v.0.3.1) (Table S1). Correspondingly, LoF variants in *GNB5* are underrepresented in comparison to expectation in this database; specifically, ExAC reports 8 LoF variants whereas 19 were expected. The c.242C>T (p.Ser81Leu) missense variant identified in family E, of Moroccan ancestry, and family F, of Brazilian ancestry, has a MAF $< 5 \times 10^{-5}$ (6/121,000) in the human population and 4.3×10^{-4} in Latinos (5/11,574). A sample of individuals from Morocco identified a prevalence of 1 out of 1,260 (7.94×10^{-4}) for this allele. We estimated the prevalence of the c.242C>T (p.Ser81Leu) variant in the Moroccan population by genotyping a total of 630 Moroccan individuals, including 394 Moroccans and 235 Dutch citizens of Moroccan descent by real-time PCR. Pathogenicity of this variant is further supported by three-dimensional representation of the encoded protein complexed with RGS9, a member of the R7 subfamily of regulators of G-protein signaling (RGS) proteins and common binding partner of GNB5. GNB5 is folded into essentially identical seven-bladed β-propellers (WD40 repeated domains) with equivalent N-terminal helical extensions.[11] Replacement of the evolutionarily conserved serine 81 (Figure S1B) by leucine will induce localized structural changes in the immediate vicinity of this residue, which could impair both the central pore of the β-propeller and the binding kinetics of RGS proteins (Figures S3– S5).

In line with the clinical presentation of affected individuals, *Gnb5* ablation in mice resulted in marked neurobehavioral abnormalities, including learning deficiencies, hyperactivity, impaired gross motor coordination, abnormal gait,[12] defective visual adaptation,[13] and perturbed development and functioning of retinal bipolar cells.[14] Correspondingly, mice lacking *Rgs6*, the *GNB5*-dependent RGS protein enriched in heart tissue, exhibit bradycardia and hypersensitivity to parasympathomimetics.[15,16] To independently investigate the functional effects of variation of *GNB5* in the full phenotypic spectrum of subjects reported herein, we engineered a zebrafish model knocked out for *gnb5*.

CRISPR/Cas9 genome editing was used to generate zebrafish with LoF mutations in *gnb5a* and *gnb5b*. This teleost has two *GNB5* paralogs as a result of an ancient genome duplication event[17] (Figure S6). We identified stable lines with a 7 bp insertion in *gnb5a* and a 8 bp deletion and 15 bp insertion in *gnb5b*, causing a frameshift and premature truncation of the encoded proteins, respectively (Figure S7). It was anticipated that *gnb5a* and *gnb5b* might have redundant functions, which was confirmed by the absence of overt phenotypes in embryos homozygous for either LoF mutations. As a consequence, a double knockout was generated to ensure complete loss of functional Gnb5. In-crosses of *gnb5a* and *gnb5b* double heterozygotes resulted in clutches of embryos containing the expected 6.25% of $gnb5a^{-/-}/gnb5b^{-/-}$ double mutants (henceforth referred to as *gnb5* mutants). Consistent with syndrome manifestations of affected individuals, zebrafish mutant embryos had no striking dysmorphologic features (Figure S7D). However, the larvae showed impaired swimming activity, remained small, and generally died 7–14 days post fertilization (dpf), most likely as a result of their inability to feed.

To assess the putative involvement of *GNB5* in autonomic nervous system functions, we investigated the GNB5-RGS-GIRK channel pathway. As GNB5 recruits RGS proteins to G protein-coupled inward rectifier potassium (GIRK) channels involved in the hyperpolarization of cell membranes,[16,18] we investigated whether LoF of *GNB5* could delay GIRK channel deactivation kinetics, increase hyperpolarization time of cell membranes, and impair cell responsiveness to new stimuli. Carbachol (PubChem CID: 5831) is a parasympathomimetic compound that activates acetylcholine receptors of the heart and the GNB5-RGS-GIRK channel pathway. Treatment of *gnb5* mutant larvae with carbachol resulted in a strong decrease of the heart rate, whereas it had little effect on wild-type and sibling larvae (Figure 2), consistent with loss of negative regulation of

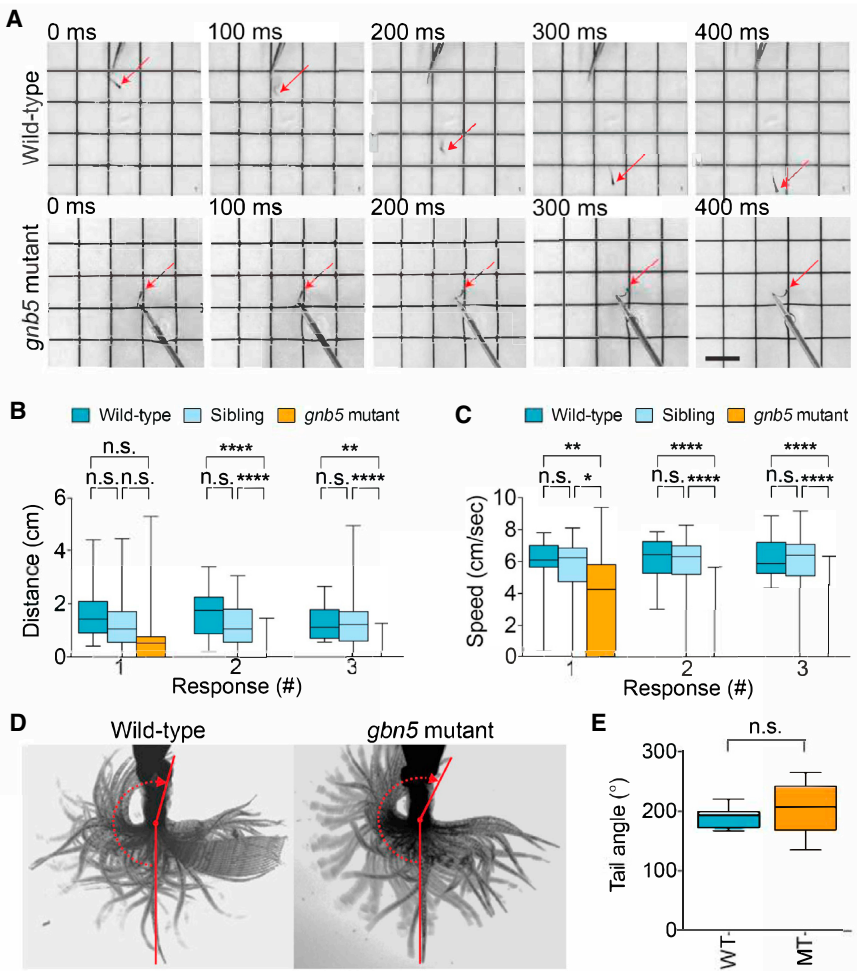

Figure 3. Neurologic Function in *gnb5* Mutant Zebrafish

(A–C) Touch-evoked escape response assay in which three consecutive tactile stimuli were applied. Embryos at 3 dpf were placed in the middle of a standard 88 mm petri dish containing E3 medium. Three consecutive tactile stimuli were applied by touching the tail of the embryo with an insect pin. Stimuli were only applied when the embryo was still. Behavior was recorded with a standard camera (30 fps) and analyzed with ImageJ (NIH) and the plugin MTrackJ.[19] (A) shows representative responses of 3 dpf wild-type and *gnb5* mutant embryos to a touch stimulus. Scale bar, 0.5 cm. Box-whisker plots show quantification of the (B) swimming distance and (C) swimming speed in TL wild-types (n = 19), siblings (n = 46), and *gnb5* mutants (n = 27).

(D and E) Analysis of maximum tail movement at 5 dpf. Larvae at 5 dpf were sedated in E3 containing 16 mg/ml Tricaine and embedded in 0.5% UltraPureTM agarose (Invitrogen 16500-500) in a 35 mm glass bottom dish. After setting, the agarose was cut away caudal to the swimming bladder, leaving the tail free to move. The dish was filled with E3 medium and embryos were left to recover from the sedation for 10 min at 28°C. Next, a maximal escape response was elicited by repeatedly touching the head of the embryo with an insect pin. Recordings were performed at 280 fps, for 30 s, with a high-speed CCD camera (Hamamatsu Photonics K.K., C9300-221) and analyzed with ImageJ (angle tool). (D) shows representative minimum projection images of tail movement in wild-type and *gnb5* mutant embryos, including tail angle analysis. The tail angle represents the angle between the head-tail midline axis in resting state and a line that was drawn from just caudal of the swimbladder to the tip of the tail at maximal tail movement. (E) Tail angle quantification is displayed in box-whisker plots (wild-type n = 10, *gnb5* mutants n = 10). fps, frames per second.

n denotes the number of fish used per dataset. Differences between two groups were analyzed via the Student's t test. Differences between more than two groups were analyzed via one-way ANOVA with Tukey's post-hoc test. Data are shown as mean ± SEM, and $p < 0.05$ was considered significant. *$p < 0.05$, **$p \leq 0.01$, ***$p \leq 0.001$, ****$p \leq 0.0001$. $p > 0.05$ was considered not significant (n.s.).

the cardiac GIRK channel by GNB5-RGS. In contrast, treatment with the sympathetic agonist isoproterenol resulted in an increased heart rate that was similar in wild-type, sibling, and *gnb5* mutant larvae (Figure 2). These results indicate that *GNB5* is crucial for parasympathetic control of heart rate, but not for sympathetic control, suggesting that lack of *GNB5* is associated with extreme bradycardia at rest. Correspondingly, affected individuals present with severe bradycardia at rest (minimal observed heart rates of <25 bpm [beats per minute]) combined with a normal chronotropic response (maximum heart rates >150 bpm).

The severe muscle hypotonia reported in affected individuals could result from GIRK-mediated hyperpolarization of neurons controlling skeletal muscle tone. *gnb5* mutant embryos hatched normally from their chorion, a process that requires muscle contraction, but their swimming behavior appeared abnormal at 3 dpf. To investigate whether this abnormal behavior was linked to neurologic dysfunction and hypotonia, we examined the touch-evoked escape response. We anticipated that neurons would only become fully hyperpolarized after an initial stimulus and thus presented the embryos with three consecutive tactile stimuli. Whereas wild-type larvae rapidly swam away in response to repeated tactile stimuli, *gnb5* mutants showed a significant decrease in swimming distance and swimming speed at stimuli two ($p \leq 0.0001$) and three ($p \leq 0.01$), but not after the first stimulus (Figures 3A–3C). Accordingly, *gnb5* mutant larvae were predominantly unresponsive to repeated tactile stimuli (Movies S1 and S2). To test whether this abnormal escape response is the consequence of neurologic dysfunction rather than reduced muscle function, we performed a tail movement assay. 5 dpf larvae were given a strong tactile stimulus while we recorded the movement of the tail (Figures 3D and 3E). No significant difference in the maximum tail angle was detected between wild-type and *gnb5* mutant larvae (Figure 3E). These results indicate that the tail muscles of *gnb5* mutants are fully functional

and that the abnormal escape response is associated with neurological dysfunction and possibly muscle hypotonia.

Given that affected individuals have visual problems, including nystagmus, we investigated the visual system by measuring the optokinetic response (OKR) of *gnb5* mutant larvae. When wild-type larvae were placed in a drum with a rotating light stimulus (Figure S8A), the OKR consisted of smooth pursuit eye movements followed by rapid rest saccades in the opposite direction (Figure S8B, Movie S3). In contrast, OKR was completely absent in *gnb5* mutant larvae although their eyes showed no morphological abnormalities and could make eye movements (Figure S8C, Movie S4). This indicates that the eye muscles are functional in *gnb5* mutants but that proper eye-movement control depends on *GNB5*. Overall these data show that *gnb5* mutants faithfully recapitulate the phenotypic spectrum of affected individuals, including cardiac, neurologic, and ophthalmologic abnormalities.

These results provide evidence for a direct role of *GNB5* in the control of heart rate, motor capacity, and vision. Whereas *GNB1* (MIM: 139380), *GNB2* (MIM: 139390), *GNB3* (MIM: 139130), and *GNB4* (MIM: 610863) are widely expressed and encode highly homologous proteins,[20] *GNB5* is preferentially expressed in the brain and nervous system and encodes a peptide with less homology with its four paralogs.[21,22]

Germline de novo *GNB1* variants cause severe neurodevelopmental disability,[23] hypotonia, and seizures. *GNB3* bi-allelic LoF has been linked to congenital stationary night blindness (MIM: 610445, 163500, 610444, 613830, 616389, 310500, 257270, 613216, 614565, 615058, 300071, and 610427) and recessive retinopathy in humans,[24,25] retinal degeneration in chickens,[26] and reduced cone sensitivity and mild bradycardia in mice.[27,28] A SNP in *GNB3* was associated with postural tachycardia syndrome[29] and incidence of cardiovascular disease and stroke.[30] Similarly, *GNB2* and *GNB4* map to loci governing heart rate on chromosomes 7 and 3, respectively.[31,32] We hereby demonstrate that bi-allelic LoF and missense variants in *GNB5* cause a multisystem syndrome with features that include global developmental delay, sinus-node dysfunction, seizures, eye abnormalities, gastric problems, and generalized hypotonia. We highlight the importance of *GNB5* for neuronal signaling, including the regulation of the antagonistic effects of the parasympathetic and sympathetic nervous system.

Supplemental Data

Supplemental Data includes Supplemental Acknowledgments, a Supplemental Note, eight figures, one table, and four movies and can be found with this article online at http://dx.doi.org/10.1016/j.ajhg.2016.06.025.

Conflicts of Interest

J.R.L. has stock ownership in 23andMe, is a paid consultant for Regeneron Pharmaceuticals, has stock options in Lasergen, is a member of the Scientific Advisory Board of Baylor Miraca Genetics Laboratories, and is a co-inventor on multiple United States and European patents related to molecular diagnostics for inherited neuropathies, eye diseases, and bacterial genomic fingerprinting. Baylor College of Medicine (BCM) and Miraca Holdings have formed a joint venture with shared ownership and governance of the Baylor Miraca Genetics Laboratories (BMGL), which performs clinical exome sequencing. The Department of Molecular and Human Genetics at BCM derives revenue from the chromosomal microarray analysis and clinical exome sequencing offered in the BMGL (http://www.bmgl.com/BMGL/Default.aspx/website). G.M. is a paid consultant for Takeda Pharmaceutical Company.

Received: May 18, 2016
Accepted: June 24, 2016
Published: August 11, 2016; corrected online: September 1, 2016

Web Resources

1000 Genomes, http://www.1000genomes.org
Berkeley Drosophila Genome Project NNSplice 0.9, http://www.fruitfly.org/seq_tools/splice.html
Burrows-Wheeler Aligner, http://bio-bwa.sourceforge.net/
dbSNP, http://www.ncbi.nlm.nih.gov/projects/SNP/
Ensembl Genome Browser, human genome, GRCh37, http://grch37.ensembl.org/Homo_sapiens/Info/Index
ExAC Browser, http://exac.broadinstitute.org/
ExomeDepth, https://cran.r-project.org/web/packages/ExomeDepth/index.html
GATK, https://www.broadinstitute.org/gatk/
GenBank, http://www.ncbi.nlm.nih.gov/genbank/
GraphPad, http://graphpad.com/
NetGene2, http://www.cbs.dtu.dk/services/NetGene2
NHLBI Exome Sequencing Project (ESP) Exome Variant Server, http://evs.gs.washington.edu/EVS/
OMIM, http://www.omim.org/
PolyPhen-2, http://genetics.bwh.harvard.edu/pph2/
PubChem, http://www.ncbi.nlm.nih.gov/pccompound
SIFT, http://sift.jcvi.org/
SnpEff, http://snpeff.sourceforge.net/
SOAPsnp, http://soap.genomics.org.cn/soapsnp.html
Swiss PDB Viewer, http://www.expasy.org/spdbv/
UMD-Predictor, http://umd-predictor.eu/

References

1. Daly, A.F., Lysy, P.A., Desfilles, C., Rostomyan, L., Mohamed, A., Caberg, J.H., Raverot, V., Castermans, E., Marbaix, E., Maiter, D., et al. (2016). GHRH excess and blockade in X-LAG syndrome. Endocr. Relat. Cancer *23*, 161–170.
2. Daly, A.F., Yuan, B., Fina, F., Caberg, J.H., Trivellin, G., Rostomyan, L., de Herder, W.W., Naves, L.A., Metzger, D., Cuny, T., et al. (2016). Somatic mosaicism underlies X-linked acrogigantism syndrome in sporadic male subjects. Endocr. Relat. Cancer *23*, 221–233.
3. Trivellin, G., Daly, A.F., Faucz, F.R., Yuan, B., Rostomyan, L., Larco, D.O., Schernthaner-Reiter, M.H., Szarek, E., Leal, L.F., Caberg, J.H., et al. (2014). Gigantism and acromegaly due to Xq26 microduplications and GPR101 mutation. N. Engl. J. Med. *371*, 2363–2374.

4. Krishnan, A., Mustafa, A., Almén, M.S., Fredriksson, R., Williams, M.J., and Schiöth, H.B. (2015). Evolutionary hierarchy of vertebrate-like heterotrimeric G protein families. Mol. Phylogenet. Evol. *91*, 27–40.
5. Alfaiz, A.A., Micale, L., Mandriani, B., Augello, B., Pellico, M.T., Chrast, J., Xenarios, I., Zelante, L., Merla, G., and Reymond, A. (2014). TBC1D7 mutations are associated with intellectual disability, macrocrania, patellar dislocation, and celiac disease. Hum. Mutat. *35*, 447–451.
6. Borck, G., Hög, F., Dentici, M.L., Tan, P.L., Sowada, N., Medeira, A., Gueneau, L., Holger, T., Kousi, M., Lepri, F., et al. (2015). BRF1 mutations alter RNA polymerase III-dependent transcription and cause neurodevelopmental anomalies. Genome Res. *25*, 609.
7. Yuan, B., Pehlivan, D., Karaca, E., Patel, N., Charng, W.L., Gambin, T., Gonzaga-Jauregui, C., Sutton, V.R., Yesil, G., Bozdogan, S.T., et al. (2015). Global transcriptional disturbances underlie Cornelia de Lange syndrome and related phenotypes. J. Clin. Invest. *125*, 636–651.
8. Ng, P.C., and Henikoff, S. (2001). Predicting deleterious amino acid substitutions. Genome Res. *11*, 863–874.
9. Adzhubei, I.A., Schmidt, S., Peshkin, L., Ramensky, V.E., Gerasimova, A., Bork, P., Kondrashov, A.S., and Sunyaev, S.R. (2010). A method and server for predicting damaging missense mutations. Nat. Methods *7*, 248–249.
10. Salgado, D., Desvignes, J.P., Rai, G., Blanchard, A., Miltgen, M., Pinard, A., Lévy, N., Collod-Béroud, G., and Béroud, C. (2016). UMD-Predictor: A High-Throughput Sequencing Compliant System for Pathogenicity Prediction of any Human cDNA Substitution. Hum. Mutat. *37*, 439–446.
11. Cheever, M.L., Snyder, J.T., Gershburg, S., Siderovski, D.P., Harden, T.K., and Sondek, J. (2008). Crystal structure of the multifunctional Gbeta5-RGS9 complex. Nat. Struct. Mol. Biol. *15*, 155–162.
12. Zhang, J.H., Pandey, M., Seigneur, E.M., Panicker, L.M., Koo, L., Schwartz, O.M., Chen, W., Chen, C.K., and Simonds, W.F. (2011). Knockout of G protein β5 impairs brain development and causes multiple neurologic abnormalities in mice. J. Neurochem. *119*, 544–554.
13. Krispel, C.M., Chen, C.K., Simon, M.I., and Burns, M.E. (2003). Novel form of adaptation in mouse retinal rods speeds recovery of phototransduction. J. Gen. Physiol. *122*, 703–712.
14. Rao, A., Dallman, R., Henderson, S., and Chen, C.K. (2007). Gbeta5 is required for normal light responses and morphology of retinal ON-bipolar cells. J. Neurosci. *27*, 14199–14204.
15. Yang, J., Huang, J., Maity, B., Gao, Z., Lorca, R.A., Gudmundsson, H., Li, J., Stewart, A., Swaminathan, P.D., Ibeawuchi, S.R., et al. (2010). RGS6, a modulator of parasympathetic activation in heart. Circ. Res. *107*, 1345–1349.
16. Posokhova, E., Wydeven, N., Allen, K.L., Wickman, K., and Martemyanov, K.A. (2010). RGS6/Gβ5 complex accelerates IKACh gating kinetics in atrial myocytes and modulates parasympathetic regulation of heart rate. Circ. Res. *107*, 1350–1354.
17. Meyer, A., and Schartl, M. (1999). Gene and genome duplications in vertebrates: the one-to-four (-to-eight in fish) rule and the evolution of novel gene functions. Curr. Opin. Cell Biol. *11*, 699–704.
18. Xie, K., Allen, K.L., Kourrich, S., Colón-Saez, J., Thomas, M.J., Wickman, K., and Martemyanov, K.A. (2010). Gbeta5 recruits R7 RGS proteins to GIRK channels to regulate the timing of neuronal inhibitory signaling. Nat. Neurosci. *13*, 661–663.
19. Meijering, E., Dzyubachyk, O., and Smal, I. (2012). Methods for cell and particle tracking. Methods Enzymol. *504*, 183–200.
20. Gautam, N., Downes, G.B., Yan, K., and Kisselev, O. (1998). The G-protein betagamma complex. Cell. Signal. *10*, 447–455.
21. Watson, A.J., Katz, A., and Simon, M.I. (1994). A fifth member of the mammalian G-protein beta-subunit family. Expression in brain and activation of the beta 2 isotype of phospholipase C. J. Biol. Chem. *269*, 22150–22156.
22. Witherow, D.S., and Slepak, V.Z. (2003). A novel kind of G protein heterodimer: the G beta5-RGS complex. Receptors Channels *9*, 205–212.
23. Petrovski, S., Kury, S., Myers, C.T., Anyane-Yeboa, K., Cogne, B., Bialer, M., Xia, F., Hemati, P., Riviello, J., Mehaffey, M., et al. (2016). Germline De Novo Mutations in GNB1 Cause Severe Neurodevelopmental Disability, Hypotonia, and Seizures. American journal of human genetics.
24. Vincent, A., Audo, I., Tavares, E., Maynes, J.T., Tumber, A., Wright, T., Li, S., Michiels, C., Consortium, G.N.B., Condroyer, C., et al. (2016). Biallelic Mutations in GNB3 Cause a Unique Form of Autosomal-Recessive Congenital Stationary Night Blindness. American journal of human genetics.
25. Arno, G., Holder, G.E., Chakarova, C., Kohl, S., Pontikos, N., Fiorentino, A., Plagnol, V., Cheetham, M.E., Hardcastle, A.J., Webster, A.R., et al. (2016). Recessive Retinopathy Consequent on Mutant G-Protein beta Subunit 3 (GNB3). J. Am. Med. Assoc. Ophthalmol.
26. Tummala, H., Ali, M., Getty, P., Hocking, P.M., Burt, D.W., Inglehearn, C.F., and Lester, D.H. (2006). Mutation in the guanine nucleotide-binding protein beta-3 causes retinal degeneration and embryonic mortality in chickens. Invest. Ophthalmol. Vis. Sci. *47*, 4714–4718.
27. Nikonov, S.S., Lyubarsky, A., Fina, M.E., Nikonova, E.S., Sengupta, A., Chinniah, C., Ding, X.Q., Smith, R.G., Pugh, E.N., Jr., Vardi, N., and Dhingra, A. (2013). Cones respond to light in the absence of transducin β subunit. J. Neurosci. *33*, 5182–5194.
28. Ye, Y., Sun, Z., Guo, A., Song, L.S., Grobe, J.L., and Chen, S. (2014). Ablation of the GNB3 gene in mice does not affect body weight, metabolism or blood pressure, but causes bradycardia. Cell. Signal. *26*, 2514–2520.
29. Nakao, R., Tanaka, H., Takitani, K., Kajiura, M., Okamoto, N., Kanbara, Y., and Tamai, H. (2012). GNB3 C825T polymorphism is associated with postural tachycardia syndrome in children. Pediatrics international: official journal of the Japan Pediatric Society *54*, 829–837.
30. Zhang, L., Zhang, H., Sun, K., Song, Y., Hui, R., and Huang, X. (2005). The 825C/T polymorphism of G-protein beta3 subunit gene and risk of ischaemic stroke. J. Hum. Hypertens. *19*, 709–714.
31. den Hoed, M., Eijgelsheim, M., Esko, T., Brundel, B.J., Peal, D.S., Evans, D.M., Nolte, I.M., Segrè, A.V., Holm, H., Handsaker, R.E., et al.; Global BPgen Consortium; CARDIoGRAM Consortium; PR GWAS Consortium; QRS GWAS Consortium; QT-IGC Consortium; CHARGE-AF Consortium (2013). Identification of heart rate-associated loci and their effects on cardiac conduction and rhythm disorders. Nat. Genet. *45*, 621–631.
32. Smolock, E.M., Ilyushkina, I.A., Ghazalpour, A., Gerloff, J., Murashev, A.N., Lusis, A.J., and Korshunov, V.A. (2012). Genetic locus on mouse chromosome 7 controls elevated heart rate. Physiol. Genomics *44*, 689–698.